Physics Letters B 764 (2017) 282–288

Contents lists available at ScienceDirect

Physics Letters B

www.elsevier.com/locate/physletb

# Polarization and dilepton anisotropy in pion–nucleon collisions

Enrico Speranza [a,b,*], Miklós Zétényi [c,d,e], Bengt Friman [a]

[a] GSI Helmholtzzentrum für Schwerionenforschung GmbH, D-64291 Darmstadt, Germany
[b] Technische Universität Darmstadt, D-64289 Darmstadt, Germany
[c] Wigner Research Center for Physics, H-1121 Budapest, Hungary
[d] Extreme Matter Institute EMMI, GSI, D-64291 Darmstadt, Germany
[e] Institut für Theoretische Physik, Goethe-Universität, D-60438 Frankfurt am Main, Germany

ARTICLE INFO

*Article history:*
Received 31 May 2016
Received in revised form 31 October 2016
Accepted 10 November 2016
Available online 15 November 2016
Editor: V. Metag

ABSTRACT

Hadronic polarization and the related anisotropy of the dilepton angular distribution are studied for the reaction $\pi N \to Ne^+e^-$. We employ consistent effective interactions for baryon resonances up to spin-5/2, where non-physical degrees of freedom are eliminated, to compute the anisotropy coefficients for isolated intermediate baryon resonances. It is shown that the spin and parity of the intermediate baryon resonance is reflected in the angular dependence of the anisotropy coefficient. We then compute the anisotropy coefficient including the $N(1520)$ and $N(1440)$ resonances, which are essential at the collision energy of the recent data obtained by the HADES Collaboration on this reaction. We conclude that the anisotropy coefficient provides useful constraints for unraveling the resonance contributions to this process.



## 1. Introduction

Dilepton production in hadronic reactions provides information on the electromagnetic properties of hadrons. Leptons are also important probes of nuclear collisions, since their mean-free path in nuclear matter is much larger than nuclear sizes. Hence, they can carry information on the conditions that prevail during the brief, highly compressed stages of the reaction. Dileptons are produced in a variety of different elementary processes. Multiply differential cross sections for dilepton production can provide information needed to disentangle the production channels.

Independently of the specific reaction, dileptons originate from the decay of virtual photons. According to the vector meson dominance hypothesis, hadrons couple to the electromagnetic field via a neutral vector meson, which subsequently converts into a photon. Although vector meson dominance does not provide an accurate description of the electromagnetic coupling for all hadrons, it provides a tenable first approximation. This implies that dilepton production in nuclear collisions can furnish information on the in-medium spectral functions of vector mesons.

A detailed understanding of elementary hadronic reactions is an important prerequisite for studies of nuclear collisions. While a lot of effort has been invested in the study of dilepton production in nucleon–nucleon collisions both in experiment and theory, pion–nucleon collisions are less explored. The HADES Collaboration has recently studied pion-induced reactions, including dilepton production. First preliminary data have been presented at the NSTAR2015 conference [1]. The aim of the present paper is to explore the reaction $\pi N \to R \to Ne^+e^-$, where $R$ is the intermediate baryon resonance, in terms of effective Lagrangian models at the center-of-momentum (CM) energy of the HADES experiment. In particular we study the angular distribution of the produced dileptons.

The general expression for the angular distribution of dileptons originating from the decay of a virtual photon is given by [2–4]:

$$\frac{d\sigma}{d\Omega_e} \propto 1 + \lambda_\theta \cos^2\theta_e + \lambda_{\theta\phi} \sin 2\theta_e \cos\phi_e + \lambda_\phi \sin^2\theta_e \cos 2\phi_e, \quad (1)$$

where $\theta_e$ and $\phi_e$ are the polar and azimuthal angles of one of the two leptons in the rest frame of the photon. The anisotropy coefficients $\lambda_\theta$, $\lambda_{\theta\phi}$ and $\lambda_\phi$ depend on the choice of the quantization axis. We use the so-called helicity frame where the polarization axis is chosen along the momentum of the virtual photon in the CM frame [5].

As we discuss in Section 2, in the reaction $\pi N \to R \to Ne^+e^-$, the anisotropy coefficients depend on the quantum numbers of the intermediate baryon resonance and on the scattering angle $\theta_{\gamma^*}$ of

* Corresponding author.
*E-mail address:* e.speranza@gsi.de (E. Speranza).

http://dx.doi.org/10.1016/j.physletb.2016.11.015

the virtual photon. In Ref. [6] the coefficient $\lambda_\theta$ has been computed for some of the relevant dilepton sources in heavy-ion collisions. On the experimental side, a non-zero polarization of the $J/\psi$ has been found in proton–proton [7] and proton–nucleus collisions [5]. In heavy-ion collisions the anisotropy coefficients is compatible with zero at low invariant masses of the lepton pair [8].

In pion–nucleon scattering, it is expected that a major part of the dilepton production cross section is due to $s$-channel baryon resonances with a mass close to the CM energy $\sqrt{s}$. The emergence of a dilepton anisotropy in these processes can be understood as follows. The initial state, which in the CM frame contains a pion with momentum $\mathbf{p}$ and a nucleon with momentum $-\mathbf{p}$, can be expanded in terms of eigenstates of orbital angular momentum

$$|\pi(\mathbf{p}); N(-\mathbf{p})\rangle \propto \sum_{lm} Y^*_{lm}(\theta,\phi)\,|lm\rangle\,, \tag{2}$$

where $\theta$ and $\phi$ specify the direction of $\mathbf{p}$ with respect to the quantization axis. Here spin quantum numbers as well as the normalization are omitted for clarity. We choose the quantization axis $z$ parallel to the momentum of the incident pion, implying that $\theta = 0$. Since $Y_{lm}(\theta = 0, \phi) \neq 0$ only for $m = 0$, the $z$-component of the orbital angular momentum vanishes in the initial state. Hence, the projection of the total spin of the intermediate baryon resonance on the beam axis is given by the $z$-component of the nucleon spin. This means that only the $J_z = +1/2$ and $-1/2$ states of the resonance are populated.

As a result, in case of an unpolarized nucleon target, spin-1/2 intermediate resonances are unpolarized, and consequently there is no preferred direction in the CM frame. Accordingly, in this case all observables are independent of the scattering angle, i.e., the angle $\theta_{\gamma^*}$ of the virtual photon in the CM frame. On the other hand, intermediate resonances of spin $\geq 3/2$ have a nontrivial polarization, implying an angular anisotropy in the CM frame. Consequently, in this case, observables show a nontrivial dependence on the scattering angle $\theta_{\gamma^*}$, which reflects the quantum numbers of the resonance.

The determination of the quantum numbers of the baryon resonances produced in pion–nucleon collisions is important for gaining a deeper understanding of hadron–hadron interactions in general and dilepton production in hadronic collisions in particular. The above arguments indicate that the study of the angular distribution of dileptons can provide valuable information on the spin and parity of the intermediate resonances. In principle, by comparing measured angular distributions of the dileptons with theoretical predictions for different resonance states, it should be possible to set constraints on the quantum numbers of the resonance. The same idea has been used e.g. to determine the quantum numbers of the $X(3872)$ meson [9].

At the intermediate energies explored in the HADES experiment, the task is facilitated by the small number of baryon resonances that contribute significantly. However, in practice the situation is often more complex than in the ideal case of an isolated resonance which dominates the cross section. Thus, in general there is interference with nearby resonances and with a nonresonant background which must be accounted for.

In this paper we study the angular distribution of dileptons in the process $\pi N \to N e^+ e^-$ in terms of the anisotropy coefficient $\lambda_\theta$ of Eq. (1). In Section 2 we give the expressions of the differential cross section and the anisotropy coefficient. In Section 3 we briefly review the effective Lagrangian of our model. This is followed by a presentation of the numerical results for the anisotropy coefficient in Section 4, where we also briefly explore the effect of nearby resonances. Conclusions are presented in Section 5.

## 2. Cross section and anisotropy coefficient

The differential cross section of the process $\pi N \to N e^+ e^-$ can be written in the form

$$\frac{d\sigma}{dM d\cos\theta_{\gamma^*} d\Omega_e} = \frac{M}{64(2\pi)^4 s}\frac{|\mathbf{p}_f|}{|\mathbf{p}_i|}\frac{1}{n_{\rm pol}}\sum_{\rm pol}|\mathcal{M}|^2\,, \tag{3}$$

where $\mathcal{M}$ is the matrix element, $\theta_{\gamma^*}$ is the polar angle of the momentum of the virtual photon in the CM frame measured from the beam axis and $d\Omega_e$ is the solid angle of the electron in the rest frame of the lepton pair [10]. Moreover, $M$ is the invariant mass of the lepton pair, $s$ is the square of the CM energy, $\mathbf{p}_i$ and $\mathbf{p}_f$ are the CM three-momenta of the initial and final nucleons, respectively. The sum is over all spin states in the initial and final state particles and $n_{\rm pol}$ is the number of spin polarizations in the initial state.

The square of the matrix element can be written in the form

$$\sum_{\rm pol}|\mathcal{M}|^2 = \frac{e^2}{k^4}W_{\mu\nu}l^{\mu\nu}, \tag{4}$$

where the lepton tensor,

$$l^{\mu\nu} = 4\left[k_1^\mu k_2^\nu + k_1^\nu k_2^\mu - (k_1\cdot k_2 + m_e^2)g^{\mu\nu}\right] \tag{5}$$

describes the coupling of the virtual photon to the $e^+e^-$ pair, $k_1$ and $k_2$ being the momenta of the electron and positron, respectively, and $m_e$ being the electron mass. The quantity

$$W_{\mu\nu} = \sum_{\rm pol}\mathcal{M}^{\rm had}_\mu \mathcal{M}^{\rm had*}_\nu \tag{6}$$

is the hadronic tensor, where $\mathcal{M}^{\rm had}_\mu$ is the hadronic part of the matrix element $\mathcal{M}$.

The nontrivial angular distribution of the $e^+e^-$ pair is connected with the polarization state of the decaying virtual photon. Therefore it is convenient to work in the polarization density matrix representation [11]. Let $\epsilon^\mu(k,\lambda)$ denote the polarization vector of the virtual photon of momentum $k$ (the helicity $\lambda$ can take on values $\pm1$ and 0, since virtual photons can also be longitudinally polarized). The polarization vectors for the three helicities are, in the rest frame of the virtual photon,

$$\epsilon^\mu(k,-1) = \frac{1}{\sqrt{2}}(0,1,-i,0), \tag{7}$$

$$\epsilon^\mu(k,0) = (0,0,0,1), \tag{8}$$

$$\epsilon^\mu(k,+1) = -\frac{1}{\sqrt{2}}(0,1,i,0). \tag{9}$$

We define the hadronic (or production) density matrix as

$$\rho^{\rm had}_{\lambda,\lambda'} = \frac{e^2}{k^4}\epsilon^\mu(k,\lambda)W_{\mu\nu}\epsilon^\nu(k,\lambda')^* \tag{10}$$

and the leptonic (or decay) density matrix as

$$\rho^{\rm lep}_{\lambda',\lambda} = \epsilon^\mu(k,\lambda')l_{\mu\nu}\epsilon^\nu(k,\lambda)^*. \tag{11}$$

In terms of the density matrices the square of the matrix element is given by

$$\sum_{\rm pol}|\mathcal{M}|^2 = \sum_{\lambda,\lambda'}\rho^{\rm had}_{\lambda,\lambda'}\rho^{\rm lep}_{\lambda',\lambda}. \tag{12}$$

The equivalence of Eqs. (4) and (12) is seen by employing the identity

$$\sum_{\lambda} \epsilon^{\mu}(k,\lambda)\epsilon^{\nu}(k,\lambda)^{*} = -g^{\mu\nu} + \frac{k^{\mu}k^{\nu}}{k^{2}} \tag{13}$$

and the fact that $k^{\mu} l_{\mu\nu} = 0$.

The explicit form of the lepton spin density matrix $\rho^{\rm lep}_{\lambda',\lambda}$ is given by

$$\rho^{\rm lep}_{\lambda',\lambda} = 4|\mathbf{k}_1|^2 \begin{pmatrix} 1+\cos^2\theta_e+\alpha & -\sqrt{2}\cos\theta_e\sin\theta_e e^{-i\phi_e} & \sin^2\theta_e e^{-2i\phi_e} \\ -\sqrt{2}\cos\theta_e\sin\theta_e e^{i\phi_e} & 2(1-\cos^2\theta_e)+\alpha & \sqrt{2}\cos\theta_e\sin\theta_e e^{-i\phi_e} \\ \sin^2\theta_e e^{2i\phi_e} & \sqrt{2}\cos\theta_e\sin\theta_e e^{i\phi_e} & 1+\cos^2\theta_e+\alpha \end{pmatrix}, \tag{14}$$

where $\theta_e$ and $\phi_e$ are the polar and azimuthal angle of one of the two lepton momenta relative to the polarization axis in the rest frame of the virtual photon, $\mathbf{k}_1$ is the three-momentum of one of the two leptons in the virtual photon rest frame and $\alpha = \frac{2m_e^2}{|\mathbf{k}_1|^2}$. As noted above, we use the so-called helicity frame. In the rest of the paper we neglect the electron mass. The angular dependence of the squared matrix element is obtained by combining Eqs. (12) and (14),

$$\begin{aligned}\sum_{\rm pol}|\mathcal{M}|^2 \propto{}& (1+\cos^2\theta_e)(\rho^{\rm had}_{-1,-1}+\rho^{\rm had}_{1,1}) + 2(1-\cos^2\theta_e)\rho^{\rm had}_{0,0} \\ &+ \sqrt{2}\cos\theta_e\sin\theta_e\left[e^{i\phi_e}(\rho^{\rm had}_{0,1}-\rho^{\rm had}_{-1,0}) \right. \\ &\left. + e^{-i\phi_e}(\rho^{\rm had}_{1,0}-\rho^{\rm had}_{0,-1})\right] \\ &+ \sin^2\theta_e(e^{2i\phi_e}\rho^{\rm had}_{-1,1}+e^{-2i\phi_e}\rho^{\rm had}_{1,-1}).\end{aligned} \tag{15}$$

Here we suppressed the explicit dependence of $\rho^{\rm had}_{\lambda,\lambda'}$ on $M$ and $\theta_{\gamma^*}$. By comparing Eqs. (1) and (15), we can identify the anisotropy coefficients

$$\lambda_\theta = \frac{\rho^{\rm had}_{-1,-1}+\rho^{\rm had}_{1,1}-2\rho^{\rm had}_{0,0}}{\rho^{\rm had}_{-1,-1}+\rho^{\rm had}_{1,1}+2\rho^{\rm had}_{0,0}}, \tag{16}$$

$$\lambda_{\theta\phi} = \sqrt{2}\frac{{\rm Re}(\rho^{\rm had}_{0,1}-\rho^{\rm had}_{-1,0})}{\rho^{\rm had}_{-1,-1}+\rho^{\rm had}_{1,1}+2\rho^{\rm had}_{0,0}}, \tag{17}$$

$$\lambda_{\phi} = 2\frac{{\rm Re}(\rho^{\rm had}_{-1,1})}{\rho^{\rm had}_{-1,-1}+\rho^{\rm had}_{1,1}+2\rho^{\rm had}_{0,0}}, \tag{18}$$

where we used the fact that the density matrix is hermitian. Equation (15) contains two further terms, proportional to $\sin 2\theta_e \sin\phi_e$ and $\sin^2\theta_e \sin 2\phi_e$, respectively, which in principle define two additional anisotropy coefficients. However, these two additional terms are unobservable [4].

The interpretation of the $\lambda_\theta$ coefficient becomes clear if we integrate over the azimuthal angle of the electron momentum $\phi_e$. In this case only the first two terms of Eq. (15) yield a nonzero result, and hence only the diagonal elements of $\rho^{\rm had}_{\lambda,\lambda'}$ contribute to the averaged cross section. Consequently, the angular distribution Eq. (3) can be cast in the form

$$\frac{d\sigma}{dM d\cos\theta_{\gamma^*} d\cos\theta_e} \propto \Sigma_\perp(1+\cos^2\theta_e) + \Sigma_\parallel(1-\cos^2\theta_e), \tag{19}$$

where $\Sigma_\perp = \rho^{\rm had}_{-1,-1}+\rho^{\rm had}_{1,1}$ and $\Sigma_\parallel = 2\rho^{\rm had}_{0,0}$ are the contributions of the transverse and parallel polarizations of the intermediate photon to the differential cross section. Equation (19) can be rearranged in the following way:

$$\frac{d\sigma}{dM d\cos\theta_{\gamma^*} d\cos\theta_e} \propto \mathcal{N}(1+\lambda_\theta\cos^2\theta_e), \tag{20}$$

where the anisotropy coefficient $\lambda_\theta$ is given by

$$\lambda_\theta(M,\theta_{\gamma^*}) = \frac{\Sigma_\perp-\Sigma_\parallel}{\Sigma_\perp+\Sigma_\parallel}. \tag{21}$$

Thus, the anisotropy coefficient provides information on the polarization of the virtual photon. If the virtual photon is created via the decay of an intermediate baryon resonance, then $\lambda_\theta$ (and in particular its dependence on $\theta_{\gamma^*}$) depends on the quantum numbers of the baryon resonance.

Predictions for the $\lambda_\theta$ coefficient for some dilepton sources are given in Ref. [6]. In particular for the Drell–Yan process $\lambda_\theta = +1$ (the virtual photon is completely transversely polarized), while for the pion annihilation process $\lambda_\theta = -1$ (the virtual photon is completely longitudinally polarized). In the case of a medium in thermal equilibrium, the polarization of the virtual photon, and hence the anisotropy coefficient $\lambda_\theta$, in general depends on the momentum relative to the heat bath in addition to the production mechanism [12].

## 3. The model

In the present study we first focus on the contribution of Feynman diagrams containing one baryon resonance in the $s$-channel, and set the resonance mass equal to $\sqrt{s}$. Thus, we can explore the dependence of the angular shape of the anisotropy coefficient on the quantum numbers of the intermediate state in the ideal case of an isolated on-shell resonance. We then include the relevant baryon resonances in the mass range between 1.4 and 1.68 GeV and add also the corresponding $u$-channel diagrams. Obviously, this choice of diagrams is not exhaustive. Nevertheless, it provides a first estimate of interference effects. For the interpretation of the HADES data at $\sqrt{s} = 1.49$ GeV, the nearby resonances $N(1440)$, $N(1520)$ and $N(1535)$ are expected to provide the leading contributions.

We assume that baryons couple to the electromagnetic field via an intermediate $\rho^0$ meson according to the vector meson dominance model.[1] For the $\rho^0$-photon coupling we use the gauge invariant vector meson dominance model Lagrangian [14]

$$\mathcal{L}_{\rho\gamma} = -\frac{e}{2g_\rho}F^{\mu\nu}\rho^0_{\mu\nu}, \tag{22}$$

where $F^{\mu\nu} = \partial_\mu A_\nu - \partial_\nu A_\mu$ is the electromagnetic field strength tensor and $\rho^0_{\mu\nu} = \partial_\mu\rho^0_\nu - \partial_\nu\rho^0_\mu$.

We include baryon resonances up to spin-5/2. The interaction of spin-1/2 baryons with pions and $\rho$ mesons is described by the Lagrangian densities of Ref. [10],

$$\mathcal{L}_{R_{1/2}N\pi} = -\frac{g_{RN\pi}}{m_\pi}\bar\psi_R\Gamma\gamma^\mu\vec\tau\psi_N\cdot\partial_\mu\vec\pi + {\rm h.c.}, \tag{23}$$

$$\mathcal{L}_{R_{1/2}N\rho} = \frac{g_{RN\rho}}{2m_\rho}\bar\psi_R\vec\tau\sigma^{\mu\nu}\tilde\Gamma\psi_N\cdot\vec\rho_{\mu\nu} + {\rm h.c.} \tag{24}$$

Here, and also in the Lagrangians involving higher spin resonances given below, $\Gamma = \gamma_5$ for $J^P = 1/2^+$, $3/2^-$ and $5/2^+$ resonances and $\Gamma = 1$ otherwise, and $\tilde\Gamma = \gamma_5\Gamma$.

Higher spin fermions are represented by Rarita–Schwinger spinor fields in effective Lagrangian models. These fields transform according to a product of a spin-1/2 and one or more spin-1 representations of the Lorentz group. Therefore they contain some contributions describing the propagation of lower-spin states. In

[1] We neglect the isoscalar channel, i.e. the $\omega$ meson, since it is not expected to modify the polarization of the virtual photon. We note, however, that $\rho-\omega$ interference [13] may affect the dependence of the polarization observables on the dilepton invariant mass.

a consistent Lagrangian involving higher-spin baryons, the lower-spin components of the Rarita–Schwinger fields should not contribute to observable quantities.

Such a consistent interaction scheme for spin-3/2 fermions was developed by Pascalutsa [15] and generalized for spin-5/2 fermions by Vrancx et al. [16]. In this work we specify the Lagrangian describing the interaction of higher-spin baryon resonances based on the scheme of Ref. [16]. In this scheme, the lower-spin degrees of freedom are eliminated from observables by requiring that the Lagrangian is invariant under the gauge transformations

$$\psi_\mu \to \psi_\mu + i\partial_\mu \chi, \tag{25}$$

$$\psi_{\mu\nu} \to \psi_{\mu\nu} + \frac{i}{2}(\partial_\mu \chi_\nu + \partial_\nu \chi_\mu), \tag{26}$$

for spin-3/2 ($\psi_\mu$) and spin-5/2 ($\psi_{\mu\nu}$) Rarita–Schwinger fields, respectively. In the above equations, $\chi$ and $\chi_\mu$ are arbitrary spinor and spinor-vector fields, respectively. The gauge invariance of Eqs. (25) and (26) is ensured if only the gauge invariant expressions of the fields

$$G_{\mu,\nu} = i(\partial_\mu \psi_\nu - \partial_\nu \psi_\mu), \tag{27}$$

$$G_{\mu\nu,\lambda\rho} = -\partial_\mu\partial_\nu\psi_{\lambda\rho} - \partial_\lambda\partial_\rho\psi_{\mu\nu} + \frac{1}{2}(\partial_\mu\partial_\lambda\psi_{\nu\rho} + \partial_\mu\partial_\rho\psi_{\nu\lambda} + \partial_\nu\partial_\lambda\psi_{\mu\rho} + \partial_\nu\partial_\rho\psi_{\mu\lambda}) \tag{28}$$

appear in the Lagrangian. Furthermore, by defining the fields

$$\Psi_\mu = \gamma^\nu G_{\mu,\nu}, \qquad \Psi_{\mu\nu} = \gamma^\lambda\gamma^\rho G_{\mu\nu,\lambda\rho}, \tag{29}$$

and making the replacements

$$\psi_\mu \to \frac{1}{m}\Psi_\mu, \quad \text{and} \quad \psi_{\mu\nu} \to \frac{1}{m^2}\Psi_{\mu\nu} \tag{30}$$

in a "traditional" Lagrangian containing Rarita–Schwinger fields one obtains a gauge invariant and hence consistent Lagrangian. The mass parameter $m$ in Eq. (30) is introduced for dimensional reasons.

Starting from the Lagrangians of Ref. [16] and taking the isospin structure into account, we obtain the expressions

$$\mathcal{L}_{R_{3/2}N\pi} = \frac{ig_{RN\pi}}{m_\pi^2}\bar\Psi_R^\mu \Gamma\vec\tau\psi_N\cdot\partial_\mu\vec\pi + \text{h.c.}, \tag{31}$$

$$\mathcal{L}_{R_{5/2}N\pi} = -\frac{g_{RN\pi}}{m_\pi^4}\bar\Psi_R^{\mu\nu} \Gamma\vec\tau\psi_N\cdot\partial_\mu\partial_\nu\vec\pi + \text{h.c.}, \tag{32}$$

for the Lagrangians describing the resonance-nucleon–pion interaction. In the case of $\Delta$ resonances, the Pauli matrices $\vec\tau$ appearing in the above and the following Lagrangians have to be replaced by the isospin-3/2 $\to$ 1/2 transition matrices.

The resonance-nucleon-$\rho$ interaction Lagrangian is analogous to the electromagnetic resonance-nucleon transition Lagrangian. Out of the three Lagrangians given in Ref. [16] we choose the one with the lowest number of derivatives. After including the isospin structure of the interaction, the Lagrangians are given by

$$\mathcal{L}_{R_{3/2}N\rho} = \frac{ig_{RN\rho}}{4m_\rho^2}\bar\Psi_R^\mu\vec\tau\gamma^\nu\tilde\Gamma\psi_N\cdot\vec\rho_{\nu\mu} + \text{h.c.}, \tag{33}$$

$$\mathcal{L}_{R_{5/2}N\rho} = -\frac{g_{RN\rho}}{(2m_\rho)^4}\bar\Psi_R^{\mu\nu}\vec\tau\tilde\Gamma\gamma^\rho(\partial_\mu\psi_N)\cdot\vec\rho_{\rho\nu} + \text{h.c.} \tag{34}$$

We explore the relevance of the different spins and parities by computing the anisotropy coefficient with a hypothetical resonance for each spin-parity combination, all with the same mass and width, $m_R = 1.49$ GeV and $\Gamma_R = 0.15$ GeV. The mass was chosen to coincide with the CM energy $\sqrt{s}$ used in our calculations, thus assuming that in the $s$-channel the resonance is on the mass shell.

We also made calculations including all well established resonance states in the relevant energy domain. These states are the nucleon resonances $N(1440)\ 1/2^+$, $N(1520)\ 3/2^-$, $N(1535)\ 1/2^-$, $N(1650)\ 1/2^-$, $N(1675)\ 5/2^-$, $N(1680)\ 5/2^+$, and the $\Delta$ resonances $\Delta(1600)\ 3/2^+$, and $\Delta(1620)\ 1/2^-$. The coupling constants $g_{RN\pi}$ and $g_{RN\rho}$ were determined from the widths of the $R \to N\pi$ and $R \to N\rho \to N\pi\pi$ decays. The empirical values for these partial widths were obtained as a product of the total width and the appropriate branching ratio as given by the Particle Data Group [17]. Masses of the resonances are also taken from Ref. [17].

We stress that the present model is intended to be valid for virtual photon masses not far from the $\rho$ meson mass. The gauge invariant version of the vector meson dominance (22) does not contribute to processes with real photons and, therefore, the model has to be supplemented by a separate coupling of baryon resonances to the nucleon and photon, if we want to describe processes with low mass virtual or real photons. On the other hand, using the original (not gauge invariant) version of the vector meson dominance by Sakurai [18], the photonic branching ratios of the baryon resonances are overpredicted [19].

The $\Delta(1232)$ resonance is not included, since there is no information available on the coupling strengths to the $N\rho$ channel and its mass is far below the CM energy considered.

We use a simplifying approximation for the mass dependence of the resonance width, assuming that it is given by that of the $N\pi$ channel, and employ the parametrization of Ref. [10].

## 4. Results

We employ the model described above to compute the anisotropy coefficient $\lambda_\theta$ of Eq. (21) for the reaction $\pi N \to Ne^+e^-$. In the following we discuss the dependence of the anisotropy coefficient on the polar angle of the virtual photon $\theta_{\gamma^*}$. In all the calculations, the CM energy is set to $\sqrt{s} = 1.49$ GeV, corresponding to the HADES data.

In order to demonstrate the effect of different spin-parity baryon resonance states on the $\lambda_\theta$ coefficient, we first use the model with the hypothetical resonances discussed above, including only the $s$-channel Feynman diagram. In Fig. 1 we show the anisotropy coefficient for dileptons of invariant mass $M = 0.5$ GeV. In this case the resonance in the intermediate state is on-shell and, therefore, the results should correspond to standard angular momentum coupling. Fig. 1 shows that the spin and parity of the intermediate resonance is reflected in a characteristic angular dependence of the anisotropy coefficient. In particular, in the spin-1/2 channels the $\lambda_\theta$ coefficient is independent of $\theta_{\gamma^*}$, in accordance with the arguments given in the introduction. Based on the same arguments, the $z$-component of the total spin coincides with the $z$-component of the initial nucleon spin. Since the nucleon target is unpolarized, the $J_z = +1/2$ and $-1/2$ polarization states of each resonance are equally populated. This means that there is no preferred direction and, consequently, that the $\lambda_\theta$ coefficient is isotropic.

The dependence of the anisotropy coefficient on the quantum numbers of the intermediate baryon resonance can be interpreted in terms of angular momentum coupling, once one accounts for the fact that, in the non-relativistic limit, the off-diagonal coupling Eq. (24) is purely transverse. We note that for all channels considered, except $J^P = 1/2^+$, two values of the final state orbital angular momentum are possible. The strengths of these channels and their relative phase depend on the structure of the interac-

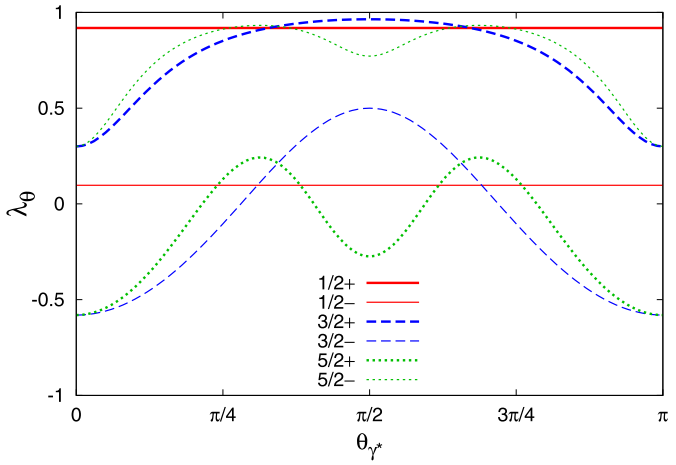


**Fig. 1.** The anisotropy coefficient $\lambda_\theta$ as a function of the virtual photon polar angle $\theta_{\gamma^*}$ for hypothetical resonance states with different spins and parities in the $s$-channel at a dilepton mass $M = 0.5$ GeV. The resonance masses coincide with $\sqrt{s} = 1.49$ GeV, the resonance widths are $\Gamma_R = 0.15$ GeV.

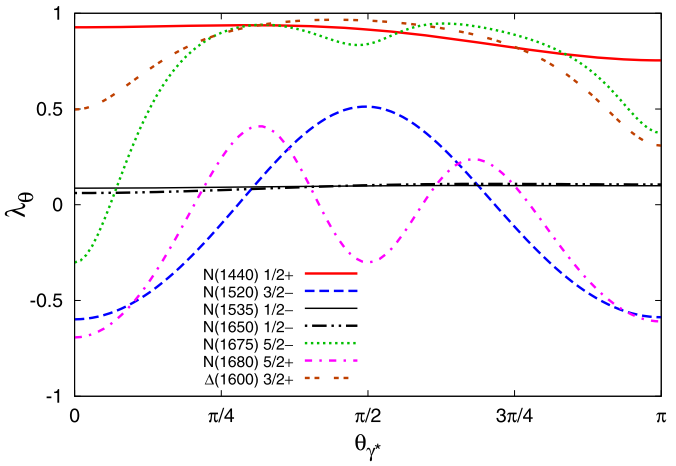


**Fig. 2.** The anisotropy coefficient $\lambda_\theta$ as a function of the virtual photon polar angle at a dilepton mass $M = 0.5$ GeV including $s$- and $u$-channel diagrams. The CM energy is $\sqrt{s} = 1.49$ GeV. For further details, see the text.

tion vertices Eqs. (24), (33), and (34). Thus, a different choice for the interaction Lagrangians [16] may lead to a somewhat different angular dependence of the anisotropy coefficient. This indicates a certain model dependence of the results. However, as long as the lowest angular momentum states dominate, we expect the results presented here to remain valid, at least on a qualitative level.

In Fig. 2 we show the $\lambda_\theta$ coefficient obtained from the $s$- and $u$-channel diagrams of seven of the physical resonance states considered. (The contribution of the $\Delta(1620)$, which has a shape very similar to the other spin-$1/2^-$ states, is left out for the sake of clarity.) Here, the characteristic shapes presented in Fig. 1 are modified mainly by the interference with the $u$-channel resonance contributions.

In order to assess which of the resonances are important for the dilepton production process at the CM energy of the HADES experiment, we compute the differential cross section $d\sigma/dM$ by integrating Eq. (3) over the scattering angle $\theta_{\gamma^*}$ and the electron solid angle $\Omega_e$. We find that at $\sqrt{s} = 1.49$ GeV and a dilepton invariant mass of $M = 0.5$ GeV, the two dominant contributions are the $N(1520)$ with $d\sigma/dM = 0.44$ μb/GeV, and the $N(1440)$ with $d\sigma/dM = 0.33$ μb/GeV. These results contain both $s$- and $u$-channel diagrams. The combined cross section taking into account both $N(1520)$ and $N(1440)$ and their interference is $d\sigma/dM = 0.84$ μb/GeV when all coupling constants are assumed to have the same phase and $d\sigma/dM = 0.70$ μb/GeV if we assume that the matrix elements involving the two resonances have the opposite phase. The range of baryon resonance widths and branching ratios given by the Particle Data Group [17] induce uncertainties in the differential cross sections. In particular, the $N(1520)$ contribution may vary by about 40%. For the $N\rho$ branching ratio of the $N(1440)$ resonance, only an upper limit is given. As a result, the combined total cross section including both the $N(1440)$ and $N(1520)$ can be up to a factor of 2 larger than the values given above. On the other extreme, the $N(1440)$ branching ratio into the $\rho N$ channel may vanish, implying that the corresponding contribution to dilepton production is negligible. Nevertheless, the average values of the branching ratios used here yield reasonable agreement with experiment, as discussed below.

The largest sub-leading contributions to the cross section are due to the $N(1535)$ and $\Delta(1600)$ resonances, which yield 0.011 μb/GeV and 0.0078 μb/GeV, respectively. Although these are negligible compared to the dominant contributions, the interference of these resonances with the dominant ones could contribute at most about ±20% in the ideal case, where the interference is either constructive or destructive throughout the whole phase space. We computed these interference terms numerically, and found that they are negligible compared to the $N(1520)$ and $N(1440)$ contributions. This remains true also when the uncertainties of the sub-leading contributions are taken into account.

Our calculation of $d\sigma/dM$ is consistent with the results of [10] at $M = 0.5$ GeV within the uncertainties discussed above. Moreover, the cross section in [10] has been compared with preliminary HADES data and found to be in a reasonable agreement at $\sqrt{s} = 1.49$ GeV and $M = 0.5$ GeV [1]. An alternative check of the reliability of the model is obtained by studying the process $\pi N \to N\pi\pi$. We thus computed the neutral $\rho$ contribution of the differential cross section at 0.5 GeV invariant mass of the pion pair, including the $N(1520)$ resonance in both the $s$- and $u$-channels. Taking the uncertainties discussed above into account, we obtain a value for $d\sigma/dM$ between 5 and 10 mb/GeV, which is consistent with the result of the partial wave analysis of the Bonn–Gatchina group, presented in [20].

The double-differential cross section, $d\sigma/dMd\cos\theta_{\gamma^*}$ obtained from $s$- and $u$-channel diagrams with the $N(1520)$ and $N(1440)$ resonances is shown in Fig. 3 as a function of the polar angle of the virtual photon, $\theta_{\gamma^*}$. Here two of the curves correspond to the contributions of the two resonances without interference. In the other two, the interference terms are included, assuming either a positive or negative relative sign between the two resonance amplitudes. In general, the interaction vertices of the resonances with pions and $\rho$ mesons can be complex, as a result of their microscopic structure [21]. This can result in an energy dependent relative phase of two resonance amplitudes between 0 and $\pi$. Since this phase is unknown, we give the results for two limiting cases, assuming a positive or negative relative sign between the $N(1520)$ and $N(1440)$ amplitudes.

From Fig. 3 it is clear that the relative phase has a strong influence on the shape of the $\theta_{\gamma^*}$ dependence of the differential cross section. Moreover, as discussed above the magnitude of the $N(1440)$ contribution is uncertain, which in turn affects the shape of the differential cross section. This suggests that the unknown phase and the coupling strength of the $N(1440)$ to the $N\rho$ channel can be constrained by data on the angular distribution.

In Fig. 4 we show the dominant contributions to the anisotropy coefficient $\lambda_\theta$ as a function of $\theta_{\gamma^*}$. As in Fig. 3, we show results for the two limiting assumptions for the relative phase of the two resonance amplitudes. In both cases, the shape of the curve

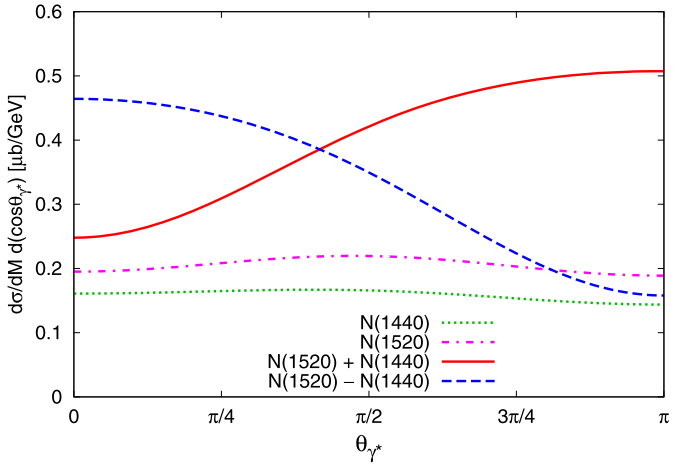


**Fig. 3.** The contribution of the two dominant resonances, $N(1440)$ and $N(1520)$, to the differential cross section of dilepton production at $\sqrt{s} = 1.49$ GeV CM energy. Two of the curves show the result obtained from $s$- and $u$-channel diagrams of each resonance. The other two curves are obtained from the sum of all four diagrams ($s$- and $u$-channel diagrams of both resonances), assuming a positive and negative relative sign between the amplitudes of the two resonances.

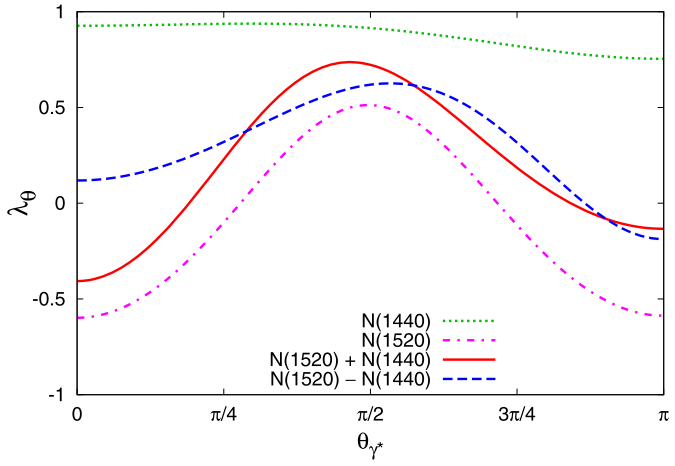


**Fig. 4.** The contribution of the two dominant resonances, $N(1440)$ and $N(1520)$, to the anisotropy coefficient, $\lambda_\theta$ at $\sqrt{s} = 1.49$ GeV CM energy. The various curves correspond to the same assumptions as in Fig. 3.

approximately follows that of the $N(1520)$ contribution, which implies that it is only weakly affected by the uncertainties of the $N(1440)$ parameters. The anisotropy parameter $\lambda_\theta$ has a maximum around $\theta_{\gamma^*} = \pi/2$. Thus, virtual photons emitted perpendicular to the beam axis in the CM frame tend to be transversely polarized, while virtual photons emitted along the beam direction are almost unpolarized or, in the case of a positive relative phase between the two resonances, photons traveling in the forward direction tend to be longitudinally polarized.

Dileptons with a low invariant mass originate from the decay of a virtual photon which is close to its mass shell. Such virtual photons must be predominantly transversely polarized. Consequently the $\lambda_\theta$ coefficient of the resulting dileptons is close to unity. This can be seen in Fig. 5, where we show the $\theta_{\gamma^*}$ dependence of the $\lambda_\theta$ coefficient for various values of the dilepton invariant mass. These results include the $s$- and $u$-channel diagrams of the dominant $N(1520)$ and $N(1440)$ resonances, assuming a positive relative sign between the amplitudes.

The anisotropy coefficient $\lambda_\theta$ can be determined experimentally by employing Eq. (20). Clearly this is very challenging, since such

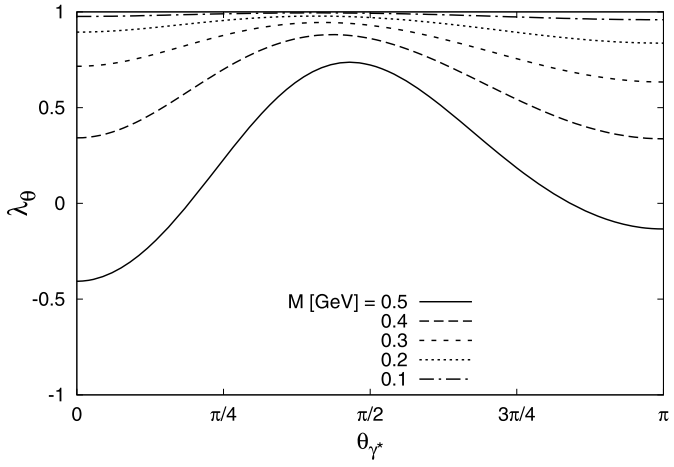


**Fig. 5.** The anisotropy coefficient $\lambda_\theta$ as a function of the virtual photon polar angle for various dilepton masses. The contributions of $s$- and $u$-channel diagrams of the two dominant resonances $N(1440)$ and $N(1520)$ and their interference term (with a positive relative sign) are included. The CM energy is $\sqrt{s} = 1.49$ GeV.

an analysis requires a triple-differential dilepton production cross section. For a fixed invariant mass $M$ and scattering angle $\theta_{\gamma^*}$, the $\lambda_\theta$ coefficient is obtained by extracting the dependence of the cross section on the electron angle $\cos^2\theta_e$. Nevertheless, the results shown in Fig. 5 suggest that a rough binning both in $M$ and $\theta_{\gamma^*}$, e.g. $M > 0.3$ GeV and three bins in $\theta_{\gamma^*}$, would be sufficient for extracting interesting information on the polarization observable.

## 5. Summary and outlook

In this paper we studied the angular distribution of dileptons originating from the process $\pi N \to N e^+ e^-$ and presented numerical results for the anisotropy coefficient $\lambda_\theta$ based on the assumption that the process is dominated by intermediate baryon resonances. We employed effective Lagrangians to describe the interactions of baryon resonances with pions and photons. The coupling of the electromagnetic field to the baryon resonances is based on the vector meson dominance model.

The coupling constants of the model have been determined using information given by the Particle Data Group [17]. Since the decay parameters of some of the baryon resonances are not very well known, our model contains uncertainties. However, the differential cross sections obtained using our model are in reasonable agreement with preliminary HADES data on dilepton production, and results on the neutral $\rho$ contribution extracted from a partial wave analysis of pion pair production. The shape of the anisotropy coefficient $\lambda_\theta$ as a function of the scattering angle is determined mainly by the $N(1520)$ resonance and hence it depends only weakly on the uncertainties of the model.

The anisotropy coefficient can in principle be determined in experiments by the HADES Collaboration at GSI, Darmstadt. To this end, at least a rough binning of the triple-differential dilepton production cross section is needed. This requires high statistics, which is not easily achieved for such a rare probe. On the other hand, as we argued in this letter, the angular distributions provide valuable additional information, which can help disentangle the various contributions to the dilepton production cross section and thus also provide novel information on the properties of baryon resonances. Consequently, high statistics data on pion induced dilepton production would provide important constraints on the elementary dilepton production mechanism as well as on the structure of baryons.

The calculation presented here is clearly exploratory. In future studies, several aspects of the model should be improved. First of all the model dependence of the predictions needs to be addressed. This can be done e.g. by repeating the calculation with different effective Lagrangians. A complementary approach, formulated in terms of helicity amplitudes or partial wave amplitudes, could provide a systematic framework for exploring the various contributions to the scattering amplitude.

A previous study suggests that at the CM energy of the HADES experiment a major part of the pion photoproduction cross section is probably due to non-resonant Born contributions [10]. Consequently, these Born terms may significantly influence also the angular distributions of dilepton production and the anisotropy coefficient in pion–nucleon collisions. Thus, their contribution to $\lambda_\theta$ should be assessed.

It is also known that the standard vector meson dominance model does not provide a satisfactory description of the electromagnetic interaction of baryon resonances. This can be improved e.g. by relaxing the universal coupling assumption [14] for the photon coupling to baryons, as discussed e.g. in Ref. [10].

Additional constraints on the model are provided by pion–nucleon collisions with other final states. In particular the one-pion and two-pion final states are measured at HADES with much better statistics than for the dilepton final state. Investigation of these final states in the framework of the same model would provide an independent check and a possibility to put tighter constraints on some of the parameters of the model. Two-pion production can also proceed via an intermediate $\rho$ meson, which makes this process particularly interesting in the present context.

## Acknowledgements

We wish to thank T. Galatyuk, P. Salabura, D. Rischke and W. Przygoda for valuable discussions. The work of E.S. was supported by GSI and TU Darmstadt (VH-NG-823). M.Z. was supported by the Hungarian OTKA Fund No. K109462, EMMI and HIC for FAIR. The work of B.F. was partially supported by EMMI.

## References

[1] W. Przygoda, HADES Collaboration, in: Proceedings of the 10th International Workshop on the Physics of Excited Nucleons, NSTAR2015, May 25–28, 2015, Osaka, Japan, JPS Conf. Proc. 10 (2016) 010013;
W. Przygoda (HADES Collaboration), talk presented at NSTAR2015.
[2] K. Gottfried, J.D. Jackson, Nuovo Cimento 33 (1964) 309.
[3] S. Falciano, et al., NA10 Collaboration, Z. Phys. C 31 (1986) 545.
[4] P. Faccioli, C. Lourenço, S. Seixas, H. Wöhri, Phys. Rev. D 83 (2011) 056008.
[5] I. Abt, et al., HERA-B Collaboration, Eur. Phys. J. C 60 (2009) 517.
[6] E.L. Bratkovskaya, O.V. Teryaev, V.D. Toneev, Phys. Lett. B 348 (1995) 283.
[7] R. Aaij, et al., LHCb Collaboration, Eur. Phys. J. C 73 (2013) 2631.
[8] R. Arnaldi, et al., NA60 Collaboration, Phys. Rev. Lett. 102 (2009) 222301.
[9] R. Aaij, et al., LHCb Collaboration, Phys. Rev. Lett. 110 (2013) 222001.
[10] M. Zétényi, Gy. Wolf, Phys. Rev. C 86 (2012) 065209.
[11] S.Y. Choi, T. Lee, H.S. Song, Phys. Rev. D 40 (1989) 2477.
[12] P. Hoyer, Phys. Lett. B 187 (1987) 162.
[13] M.F.M. Lutz, B. Friman, M. Soyeur, Nucl. Phys. A 713 (2003) 97.
[14] N.M. Kroll, T.D. Lee, B. Zumino, Phys. Rev. 157 (1967) 1376.
[15] V. Pascalutsa, Phys. Rev. D 58 (1998) 096002.
[16] T. Vrancx, L. De Cruz, J. Ryckebusch, P. Vancraeyveld, Phys. Rev. C 84 (2011) 045201.
[17] K.A. Olive, et al., Particle Data Group Collaboration, Chin. Phys. C 38 (2014) 090001.
[18] J.J. Sakurai, Currents and Mesons, University of Chicago Press, Chicago, 1969;
J.J. Sakurai, Ann. Phys. 11 (1960) 1.
[19] B. Friman, H.J. Pirner, Nucl. Phys. A 617 (1997) 496.
[20] W. Przygoda, HADES Collaboration, talk presented at the International Conference on the Structure of Baryons, Baryons 2016, May 16–20, 2016, Tallahassee, Florida, USA.
[21] M.F.M. Lutz, G. Wolf, B. Friman, Nucl. Phys. A 706 (2002) 431;
M.F.M. Lutz, G. Wolf, B. Friman, Nucl. Phys. A 765 (2006) 431 (Erratum).